DISPLACEMENT MEASUREMENT USING A TWO-PROBE IMPLEMENTATION OF MICROWAVE INTERFEROMETRY

A. V. Doronin, N. B. Gorev[*], I. F. Kodzhespirova, and E. N. Privalov

Department for Functional Elements of Control Systems, Institute of Technical Mechanics, National Academy of Sciences of Ukraine, 15 Leshko-Popel St., Dnepropetrovsk 49005, Ukraine

Abstract—This paper presents a two-probe implementation of microwave interferometry for displacement measurement at an unknown reflection coefficient. Theoretically, the proposed technique gives the exact value of the displacement for reflection coefficients (at the location of the probes) no greater than $1/\sqrt{2}$ and in the general case determines it to a worst-case accuracy of about 4.4% of the operating wavelength. Its experimental verification has demonstrated reasonable measurement accuracy for displacements several times as great as the operating wavelength (in real-time measurements at a free-space wavelength of 3 cm for a peak-to peak vibration amplitude of 15 cm, the maximum error in the determination of the instantaneous relative displacement and the peak-to-peak amplitude was about 3 mm and about 1 mm, respectively).

1. INTRODUCTION

Microwave interferometry is an ideal means for displacement measurement in various engineering applications such as position sensing, liquid-level gauging, vibration control, etc. This is due to its ability to provide fast noncontact measurements, applicability to dusty or smoky environments (as distinct from laser Doppler sensors [1–3] or vision-based systems using digital image processing techniques [4]), and simple hardware implementation in comparison with other microwave measuring instruments such as, for example, the step-frequency continuous-wave radar sensor [5]. In microwave

interferometry, the displacement of the object under measurement (target) is extracted from the phase shift between the signal reflected from the target and the reference signal. This phase shift can be determined from two quadrature signals. At present, the usual way to form such signals is to use special hardware incorporating a power divider and a phase-detecting processor, which is an analog [6] or a digital [7] quadrature mixer. In doing so, measures have to be taken to minimize the nonlinear phase response of the quadrature mixer, which is caused by its phase and amplitude unbalances. However, one can get quadrature signals in a much simpler way by extracting them from the output signals of two probes spaced at one eighth of the wavelength of sensing electromagnetic radiation, namely, from the currents of the semiconductor detectors connected to the probes. The expressions that relate the quadrature signals to the detector currents also include the magnitude of the complex reflection coefficient at the location of the probes, which is not known and may vary during measurements. Since the publication of the classic text by Tischer [8], there has been general agreement that the unknown reflection coefficient can be determined or eliminated only if no fewer than three probes are used (see, for example, [9]). Clearly increasing the number of probes adds complexity to the design of the measuring waveguide section and calls for a corresponding increase in the number of channels of the analog-to-digital converter (ADC), thus limiting the sampling frequency. The aim of this paper is to show that at an unknown reflection coefficient the displacement can be determined to sufficient accuracy using as few as two probes.

2. THEORETICAL ANALYSIS

Figure 1 shows a schematic of two-probe measurements. A waveguide section with a horn antenna facing the target is connected to the microwave oscillator. Two probes, 1 and 2, with square-law semiconductor detectors connected thereto are placed in the waveguide section $\lambda_g/8$ apart where λ_g is the guided operating wavelength, probe 1 being farther from the target. For this probe arrangement, the detector currents J_1 and J_2 (normalized to their values in the absence of a reflected wave) are

$$J_1 = 1 + |\Gamma|^2 + 2|\Gamma|\cos\psi, \tag{1}$$

$$J_2 = 1 + |\Gamma|^2 + 2|\Gamma|\sin\psi \tag{2}$$

where $|\Gamma|$ and ψ are the magnitude and phase of the unknown complex reflection coefficient $\Gamma = |\Gamma|e^{i\psi}$ at the location of probe 1, i.e., ψ is the phase difference between the reflected and the incident wave at
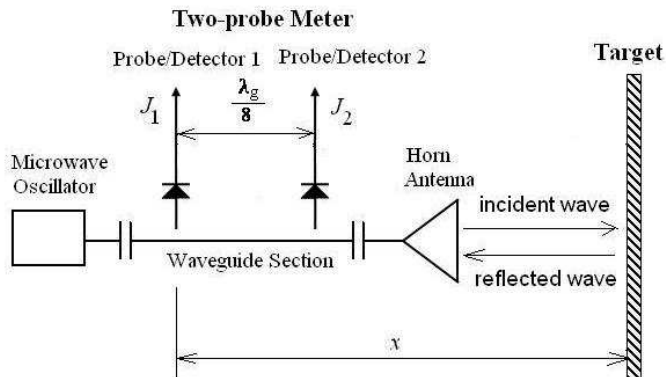
Figure 1. Schematic of two-probe measurements.

that point, and the subscripts "1" and "2" refer to probes 1 and 2, respectively (for simplicity, in the following discussion the magnitude of the complex reflection coefficient will be referred to as the reflection coefficient).

The phase difference ψ may be written as

$$\psi = \frac{4\pi x}{\lambda_0} + \phi \tag{3}$$

where x is the distance between the target and probe 1; λ_0 is the free-space operating wavelength; the term ϕ, which is governed by the waveguide section and horn antenna geometry and the phase shift caused by the reflection, does not depend on the distance x.

Let it be desired to find the displacement $\Delta x(t)$ of the target relative to its initial position $x(t_0)$ from the measured currents $J_1(t)$ and $J_2(t)$. As will be shown below, this displacement can be unambiguously determined from the quadrature signals $\cos \psi$ and $\sin \psi$. From Eqs. (1) and (2) we have

$$\cos \psi = \frac{a_1 - |\Gamma|^2}{2\,|\Gamma|}, \tag{4}$$

$$\sin \psi = \frac{a_2 - |\Gamma|^2}{2\,|\Gamma|} \tag{5}$$

where

$$a_1 = J_1 - 1, \quad a_2 = J_2 - 1. \tag{6}$$

Combining the squares of Eqs. (4) and (5) gives the biquadratic

equation in $|\Gamma|$

$$|\Gamma|^4 - (a_1 + a_2 + 2)\,|\Gamma|^2 + \frac{a_1^2 + a_2^2}{2} = 0. \tag{7}$$

This equation has two positive roots

$$|\Gamma|_1 = \left[\frac{a_1 + a_2 + 2}{2} + \sqrt{\frac{(a_1 + a_2 + 2)^2}{4} - \frac{a_1^2 + a_2^2}{2}}\,\right]^{1/2}, \tag{8}$$

$$|\Gamma|_2 = \left[\frac{a_1 + a_2 + 2}{2} - \sqrt{\frac{(a_1 + a_2 + 2)^2}{4} - \frac{a_1^2 + a_2^2}{2}}\,\right]^{1/2}, \tag{9}$$

one of which is extraneous.

Denote the positive extraneous root by $|\Gamma|_{ext}$. Using Eqs. (4) and (5), the absolute term of Eq. (7) can be brought to the form

$$\frac{a_1^2 + a_2^2}{2} = |\Gamma|^2 \left[\,|\Gamma|^2 + 2\sqrt{2}\,|\Gamma|\sin\left(\psi + \pi/4\right) + 2\right] \tag{10}$$

whence we have

$$|\Gamma|_{ext} = \left[\,|\Gamma|^2 + 2\sqrt{2}\,|\Gamma|\sin\left(\psi + \pi/4\right) + 2\right]^{1/2}. \tag{11}$$

For $|\Gamma| \leq 1/\sqrt{2}$, $|\Gamma|_{ext}$ will always be no smaller than $|\Gamma|$, and thus the reflection coefficient $|\Gamma|$ will always be given by $|\Gamma|_2$ because $|\Gamma|_2 \leq |\Gamma|_1$. For $|\Gamma| > 1/\sqrt{2}$, $|\Gamma|_{ext}$ will be smaller than $|\Gamma|$ if $\sin(\psi + \pi/4) < -1/\sqrt{2}|\Gamma|$, and thus the reflection coefficient will be given by $|\Gamma|_1$ if $\sin(\psi + \pi/4) < -1/\sqrt{2}|\Gamma|$, otherwise it will be given by $|\Gamma|_2$. For clarity, all these cases are summarized in Table 1.

First consider the case $|\Gamma| \leq 1/\sqrt{2}$. In this case, the reflection coefficient $|\Gamma|$ is unambiguously determined from Eq. (7) as its root $|\Gamma|_2$, and thus $\cos\psi$ and $\sin\psi$ are unambiguously determined from Eqs. (4) and (5). To extract the displacement of the target from $\cos\psi$ and $\sin\psi$, one can use the phase unwrapping method, which is a powerful tool to resolve the phase ambiguity problem in a variety

Table 1. The roots $|\Gamma|_1$ and $|\Gamma|_2$ of Eq. (7).

$|\Gamma| \leq 1/\sqrt{2}$	$|\Gamma| > 1/\sqrt{2}$	
	$\sin\left(\psi + \pi/4\right) < -1/\sqrt{2}\,|\Gamma|$	$\sin\left(\psi + \pi/4\right) \geq -1/\sqrt{2}\,|\Gamma|$
$|\Gamma|_1 = |\Gamma|_{ext}$	$|\Gamma|_1 = |\Gamma|$	$|\Gamma|_1 = |\Gamma|_{ext}$
$|\Gamma|_2 = |\Gamma|$	$|\Gamma|_2 = |\Gamma|_{ext}$	$|\Gamma|_2 = |\Gamma|$

of applications [6, 10, 11]. The displacement Δx of the target at time t_n, $n = 0, 1, 2, \ldots$, from its initial position $x(t_0)$ can be found by the following phase unwrapping algorithm [12]

$$\varphi(t_n) = \begin{cases} \arctan \dfrac{\sin \psi(t_n)}{\cos \psi(t_n)}, & \sin \psi(t_n) \geq 0, \quad \cos \psi(t_n) \geq 0, \\ \arctan \dfrac{\sin \psi(t_n)}{\cos \psi(t_n)} + \pi, & \cos \psi(t_n) < 0, \\ \arctan \dfrac{\sin \psi(t_n)}{\cos \psi(t_n)} + 2\pi, & \sin \psi(t_n) < 0, \quad \cos \psi(t_n) \geq 0, \end{cases} \quad (12)$$

$$\Delta\varphi(t_n) = \varphi(t_n) - \varphi(t_{n-1}), \quad (13)$$

$$\theta(t_n) = \begin{cases} 0, & n = 0, \\ \theta(t_{n-1}) + \Delta\varphi(t_n), \quad |\Delta\varphi(t_n)| \leq \pi, & n = 1, 2, \ldots, \\ \theta(t_{n-1}) + \Delta\varphi(t_n) - 2\pi \mathrm{sgn}\,[\Delta\varphi(t_n)], \quad |\Delta\varphi(t_n)| > \pi, \quad n = 1, 2, \ldots, \end{cases} \quad (14)$$

$$\Delta x(t_n) = \frac{\lambda_0}{4\pi} \theta(t_n), \qquad n = 0, 1, 2, \ldots, \quad (15)$$

where φ and θ are the wrapped and unwrapped phases, respectively.

This algorithm is applicable on condition that the phase change $\psi(t_n) - \psi(t_{n-1}) = 4[x(t_n) - x(t_{n-1})]/\lambda_0$ between two successive measurements is between $-\pi$ and π (phase changes greater than π or smaller than $-\pi$ will be interpreted as a displacement in the wrong direction, thus causing the measured displacement curve to show spurious jumps or breaks). In the assumption of harmonic vibrations of the target, the maximum change of the phase ψ between two successive measurements may be estimated as $8\pi^2 A f_{vib}/\lambda_0 f_{\mathrm{ADC}}$ where A and f_{vib} are the target vibration amplitude and frequency and f_{ADC} is the ADC sampling frequency. Because of this, the phase unwrapping algorithm will be applicable on condition that

$$\frac{8\pi^2 A f_{vib}}{\lambda_0 f_{\mathrm{ADC}}} \leq \pi \quad (16)$$

whence the minimum required ADC sampling frequency $f_{\mathrm{ADC\,min}}$ may be estimated as

$$f_{\mathrm{ADC\,min}} = \frac{8\pi A_{\max} f_{vib\,\max}}{\lambda_0} \quad (17)$$

where $A_{\max}$ and $f_{vib\,\max}$ are the maximum vibration amplitude and frequency. For example, for $A_{\max} = 7.5\,\mathrm{cm}$, $f_{vib\,\max} = 2\,\mathrm{Hz}$, and $\lambda_0 = 3\,\mathrm{cm}$ (the experiments described in the next section) $f_{\mathrm{ADC\,min}}$ is as low as $126\,\mathrm{Hz}$. However, even fast motions will present no problems for today's ADCs, whose sampling frequency is of the order of 1 GHz.

Now consider the case $|\Gamma| > 1/\sqrt{2}$. In this case, $|\Gamma|_2$ will not always be equal to $|\Gamma|$, but, as will be shown below, the displacement

can also be determined to sufficient accuracy using the root $|\Gamma|_2$ as the reflection coefficient. As discussed above, the root $|\Gamma|_2$ will be extraneous for $\sin(\psi + \pi/4) < -1/\sqrt{2}|\Gamma|$. In terms of the wrapped phase φ, this condition becomes

$$\frac{3\pi}{4} + \arcsin \frac{1}{\sqrt{2}\,|\Gamma|} < \varphi < \frac{7\pi}{4} - \arcsin \frac{1}{\sqrt{2}\,|\Gamma|} \qquad (18)$$

whence it can be seen that the wrapped phase corresponding to $\sin(\psi + \pi/4) < -1/\sqrt{2}|\Gamma|$ lies in the third quadrant. It follows from Eqs. (4) and (5) that if the root $|\Gamma|_2$ is taken as the reflection coefficient when it is extraneous, i.e., when $|\Gamma|_2 = [\,|\Gamma|^2 + 2\sqrt{2}|\Gamma| \sin(\psi + \pi/4) + 2\,]^{1/2}$, then the phase error $\Delta\varphi_{er}$ will be

$$\Delta\varphi_{er} = \arctan \frac{1 + |\Gamma| \cos \varphi}{1 + |\Gamma| \sin \varphi} + \pi - \varphi. \qquad (19)$$

It can easily be shown that the function $\Delta\varphi_{er}(\varphi)$ is zero at $\varphi = \frac{3\pi}{4} + \arcsin \frac{1}{\sqrt{2}|\Gamma|}$ and $\varphi = \frac{7\pi}{4} - \arcsin \frac{1}{\sqrt{2}|\Gamma|}$ and has a negative minimum at $\varphi_1 = \frac{3\pi}{4} + \arcsin \frac{\sqrt{2}(1+|\Gamma|^2)}{3|\Gamma|}$ and a positive maximum at $\varphi_2 = \frac{7\pi}{4} - \arcsin \frac{\sqrt{2}(1+|\Gamma|^2)}{3|\Gamma|}$, the minimum and the maximum being equal in magnitude. As can be seen from the algorithm (12)–(15), the displacement error is governed only by the phase error at the initial and the current measurement point because the intermediate points cancel one another. Because of this, at a fixed $|\Gamma|$ the maximum possible error in displacement determination will be

$$\Delta x_{er\,\max} = \frac{\lambda_0}{4\pi} \left[|\Delta\varphi_{er}(\varphi_1)| + \Delta\varphi_{er}(\varphi_2)\right] = \frac{\lambda_0}{2\pi} |\Delta\varphi_{er}(\varphi_1)|. \qquad (20)$$

Figure 2 shows the ratio $\Delta x_{er\,\max}/\lambda_0 = |\Delta\varphi_{er}(\varphi_1)|/2\pi$ versus $|\Gamma|$ for $1/\sqrt{2} < |\Gamma| \le 1$ (for $0 < |\Gamma| \le 1/\sqrt{2}$, the error $\Delta x_{er\,\max}$ is zero because $|\Gamma|_2$ is exactly equal to $|\Gamma|$). As illustrated, the maximum value of $\Delta x_{er\,\max}/\lambda_0$, which is reached at $|\Gamma| = 1$, is about 0.044, i.e., the maximum value of the error $\Delta x_{er\,\max}$ is about 4.4% of the free-space wavelength λ_0 [notice that this is the worst-case error, which occurs when the reflection coefficient is equal to unity (which is highly improbable in free-space measurements), the initial measurement point corresponds to one extremum of the function $\Delta\varphi_{er}(\varphi)$, and the current measurement point corresponds to the other]. So the reflection coefficient can always be determined to sufficient accuracy from Eq. (7) as its root $|\Gamma|_2$.

In the above discussion the interprobe distance l was assumed to be exactly equal to $\lambda_g/8$. However, in actual practice this distance
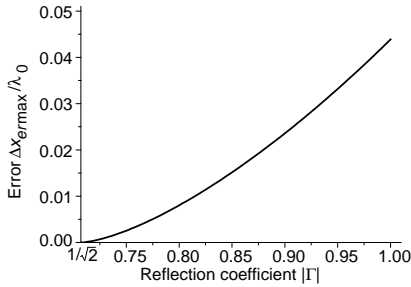
Figure 2. Maximum possible error $\Delta x_{er\,\max}$ in displacement determination versus reflection coefficient $|\Gamma|$.
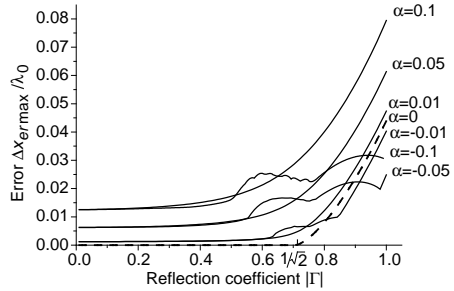
Figure 3. Effect of the interprobe distance error α on the maximum possible error $\Delta x_{er\,\max}$ in displacement determination.

is always set with some error. Let α be the relative variation of the interprobe distance l from $\lambda_g/8$, i.e., $l = \frac{\lambda_g}{8}(1 + \alpha)$. Then the current J_2 of detector 2 will be

$$J_2 = 1 + |\Gamma|^2 + 2\,|\Gamma|\sin\left(\psi - \pi\alpha/2\right), \tag{21}$$

while in the calculation of the reflection coefficient and the phase φ it is assumed that $J_2 = 1 + |\Gamma|^2 + 2|\Gamma|\sin\psi$. Thus the phase error $\Delta\varphi_{er}$ introduced by this calculation will be due both to the use of the root $|\Gamma|_2$ of Eq. (7) as the reflection coefficient when this root is extraneous and to the variation of the interprobe distance from its setting value $\lambda_g/8$

$$\Delta\varphi_{er} = \begin{cases} \varphi_{ap} - \varphi + 2\pi & \text{if} \quad 0 \leq \varphi_{ap} \leq \pi/2 \ \text{ and } 3\pi/2 \leq \varphi < 2\pi, \\ \varphi_{ap} - \varphi - 2\pi & \text{if} \quad 3\pi/2 \leq \varphi_{ap} < 2\pi \ \text{ and } 0 \leq \varphi \leq \pi/2, \\ \varphi_{ap} - \varphi & \text{otherwise} \end{cases} \tag{22}$$

where φ is the actual wrapped phase, φ_{ap} the apparent wrapped phase calculated with $J_2 = 1 + |\Gamma|^2 + 2|\Gamma|\sin(\varphi - \pi\alpha/2)$, and 2π is added or subtracted to overcome the 2π-discontinuity problem at the boundary between the first and the forth quadrant.

In this case, the maximum possible error in displacement determination will be

$$\Delta x_{er\,\max} = \frac{\lambda_0}{4\pi}\left(\Delta\varphi_{er\,\max} - \Delta\varphi_{er\,\min}\right) \tag{23}$$

where $\Delta\varphi_{er\,\max}$ and $\Delta\varphi_{er\,\min}$ are the maximum and the minimum values of the function $\Delta\varphi_{er}(\varphi)$ on the interval $0 \leq \varphi < 2\pi$.

Figure 3 shows the ratio $\Delta x_{er\,\max}/\lambda_0$ versus $|\Gamma|$ for different values of α. For comparison, the curve $\alpha = 0$ ($l = \lambda_g/8$) is shown too (dashed).

As can be seen from Figure 3, for the error $\Delta x_{er\,\max}/\lambda_0$ to be within 8 and 6% the interprobe distance error must be within 10 and 5%, respectively. A 5% distance accuracy is rather difficult to achieve mechanically, especially in the millimeter range. However, one can determine the actual interprobe distance l by electrical measurements and then operate at the frequency at which $l = \lambda_g/8$. For example, l can be determined using a short-circuiting piston ($|\Gamma| = 1$). In this case, Eqs. (1) and (21) become

$$J_1 = 2 + 2\cos\psi, \tag{24}$$
$$J_2 = 2 + 2\sin\left(\psi - \pi\alpha/2\right) \tag{25}$$

whence

$$\sin\psi = \frac{J_2 + 2\cos\psi\sin\left(\pi\alpha/2\right) - 2}{2\cos\left(\pi\alpha/2\right)}. \tag{26}$$

Let $x_{\max}$ and $x_{\min}$ be the position of the shot-circuiting piston where the current J_1 is a maximum and a minimum, respectively. Clearly $\cos\psi(x_{\max}) = 1$, $\cos\psi(x_{\min}) = -1$, and $\sin\psi(x_{\max,\,\min}) = 0$. So, from Eq. (26) we have

$$\sin\left(\pi\alpha/2\right) = \frac{2 - J_2\left(x_{\max}\right)}{2} = \frac{J_2(x_{\min}) - 2}{2}. \tag{27}$$

Under the reasonable assumption that $|\alpha| < 1$, the error α is unambiguously determined from Eq. (27).

As Eqs. (24) and (25) suggest, one more way out is to short-circuit the waveguide section ($|\Gamma| = 1$) and tune the microwave oscillator to the frequency at which the sum $[(J_1 - 2)/2]^2 + [(J_2 - 2)/2]^2$, i.e., the sum $\cos^2\psi + \sin^2(\psi - \pi\alpha/2)$ is equal to unity.

3. EXPERIMENTAL VERIFICATION

To verify the proposed technique, the displacement of a target (a brass disc or square plate) executing a vibratory motion was measured. The target was put in motion by an electrically driven crank mechanism. The measuring setup comprised a waveguide section with two probes installed therein and two semiconductor detectors connected to the probes, a horn antenna mounted at the end of the waveguide section, a microwave oscillator, a circulator with a dummy load between the microwave oscillator and the waveguide section, two amplifiers, an ADC, and a personal computer (the resonance circuits of the detectors were tuned to the microwave oscillator frequency to maximize the detector currents and extract the fundamental harmonic alone). In Figure 4, its schematic (a) is compared with that of the displacement
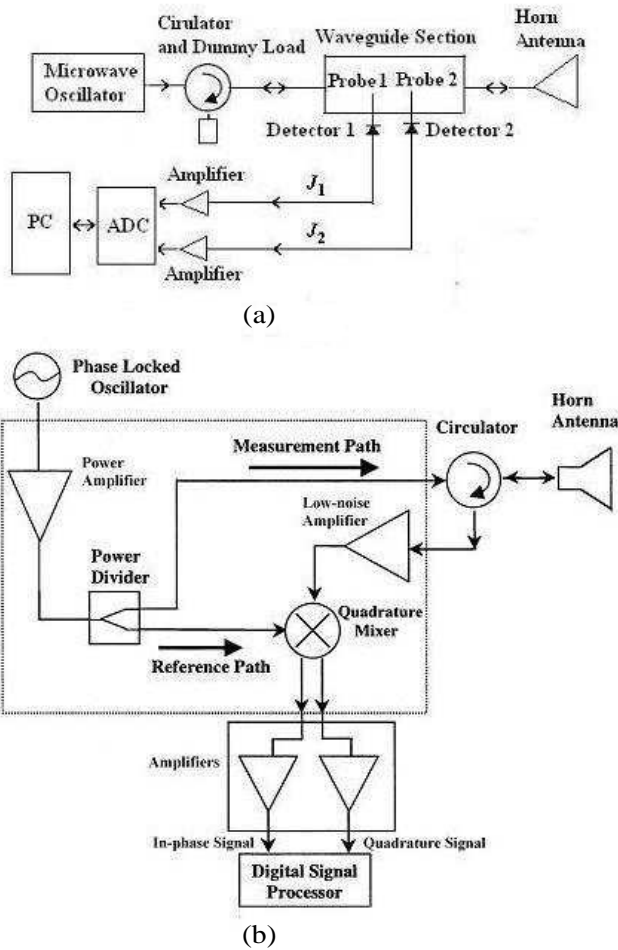
Figure 4. Schematic of (a) the measuring setup implementing the two-probe technique and of (b) the displacement sensor on the basis of a quadrature mixer [6].

sensor on the basis of a quadrature mixer [6] (b). As can be seen from the figure, the two-probe technique is far simpler in implementation.

In the experiments, the reflection coefficient was determined as the root $|\Gamma|_2$ of Eq. (7). The experiments were conducted at different values of the microwave oscillator frequency f, the peak-to-peak vibration amplitude $2A$, and the minimum distance $L_{\min}$ of the target to the antenna. Typical experimental parameters are shown in Table 2.

Figures 5, 6, and 7 show the time dependence of the target velocity,

Table 2. Typical experimental parameters.

| Experiment number	Target	f (GHz)/λ_0 (cm)	$2A$ (cm)	$L_{\min}$ (cm)
1	$\emptyset 128\,\text{mm}$ disc	10/3.00	15	100
2	$\emptyset 128\,\text{mm}$ disc	9.7/3.09	10	15
3	$70 \times 70\,\text{mm}$ square plate	9.7/3.09	10	5
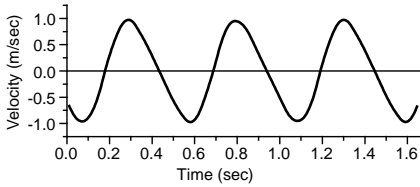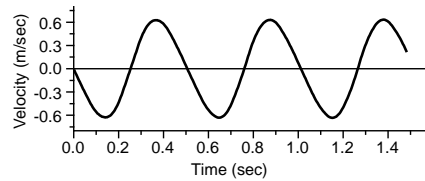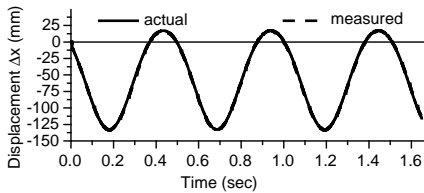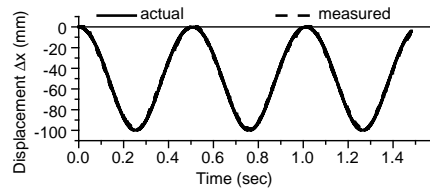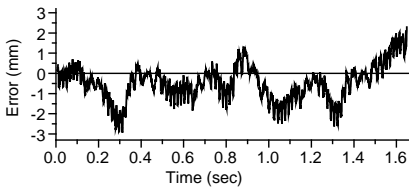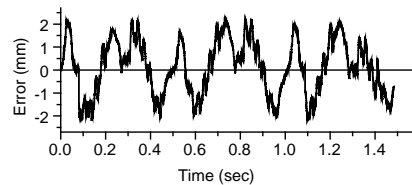
Figure 5. (a) Target velocity, (b) actual and measured displacement, and (c) displacement measurement error in Experiment 1.

Figure 6. (a) Target velocity, (b) actual and measured displacement, and (c) displacement measurement error in Experiment 2.

actual and measured displacement, and displacement measurement error for Experiments 1, 2, and 3, respectively.

The peak-to-peak amplitude was determined to an accuracy of 0.7 mm in Experiment 1, 1.1 mm in Experiment 2, and 0.2 mm in Experiment 3. The maximum and the average error in the determination of the instantaneous relative displacement was 2.9 and
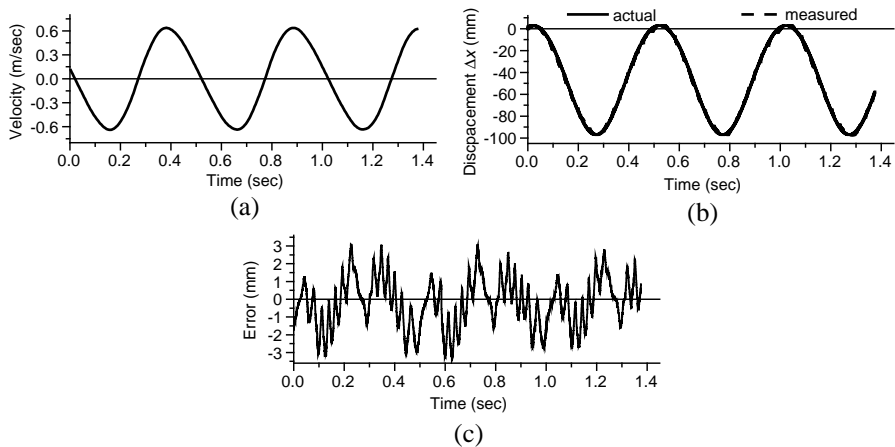
Figure 7. (a) Target velocity, (b) actual and measured displacement, and (c) displacement measurement error in Experiment 3.

0.8 mm in Experiment 1, 2.2 and 1.0 mm in Experiment 2, and 3.3 and 1.1 mm in Experiment 3. In Experiments 1 and 2, the measured reflection coefficient varied between 0.04 and 0.066 and between 0.12 and 0.62, respectively, i.e., it was less than $1/\sqrt{2} \approx 0.707$. Because of this, in these experiments the root $|\Gamma|_2$ of Eq. (7) gave the actual reflection coefficient, and thus the error was due to other factors such as deviation of the reflected wave from the plane waveform, reflections from the antenna, etc. In Experiment 3, the measured reflection coefficient varied between 0.2 and 0.76, i.e., at some of the measurement points the root $|\Gamma|_2$ might be extraneous. However, as can be seen from the figures, this did not contribute much to the error in comparison with Experiments 1 and 2. As can be seen from Figure 7, the proposed two-probe technique performs well for $L_{\min} = 5$ cm too, while the standing-wave radar proposed in [13] fails to operate at distances less than 14 cm due to positional interference of the target and the antenna.

In [6, 7], the maximum displacement measurement error was about 0.3 mm, while in this work it is about 3 mm. However, the following should be taken in consideration. The displacement measurement error may be considered as proportional to the free-space wavelength λ_0, and in [6, 7] the measurements were made at 37.6 GHz ($\lambda_0 = 8$ mm), while in this work they were made at 9.7 and 10 GHz ($\lambda_0 = 3.09$ and 3 cm). Besides, in [6, 7] the displacement was measured as the target (metal plate) was moved every 0.1 mm, and for each measurement multiple data points (1,000 data points in [7]) were sampled and averaged to cancel out noise components. In this work, the displacement of a

moving target was measured in real time, and the displacement shown in the figures was extracted from the measured data (detector currents) without any preprocessing thereof such as filtering, smoothing, etc.

The effect of the experimental parameters on the measured results was studied too. In this study, the relative error Δ in the determination of the peak-to-peak vibration amplitude $2A$ was used as the error measure. Figure 8 shows Δ versus the maximum target-to-antenna distance $L_{\max}$ (related to $L_{\min}$ as $L_{\max} = L_{\min} + 2A$) for targets in the form of 30×30, 40×40, 50×50, and $70 \times 70\,\text{mm}$ square plates ($2A = 15\,\text{cm}$ and $f = 9.7\,\text{GHz}$). As illustrated, there exists a threshold value of $L_{\max}$ above which the error sharply increases, and this threshold value increases with the target size (below the threshold, the error Δ depends only slightly on $L_{\max}$ and the target size and is within 1%). To understand this behavior of Δ, note that if the calculated phase is in error by $\Delta\varphi_{er}$, the condition (16) of the applicability of the phase unwrapping algorithm becomes

$$\frac{8\pi^2 A f_{vib}}{\lambda_0 f_{\text{ADC}}} + \Delta\varphi_{er} \leq \pi. \tag{28}$$

As the distance $L_{\max}$ increases and/or the target size decreases, the wave reflected from the target deviates from the plane waveform more and more, causing the phase error $\Delta\varphi_{er}$ to increase because the phase is calculated in the plane-wave approximation. Eventually there
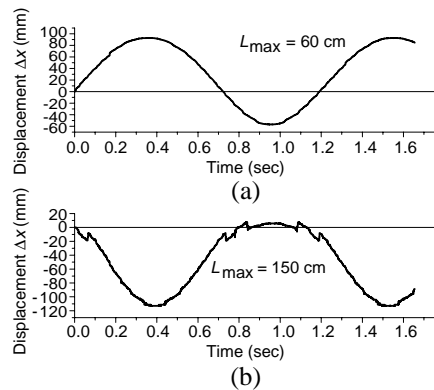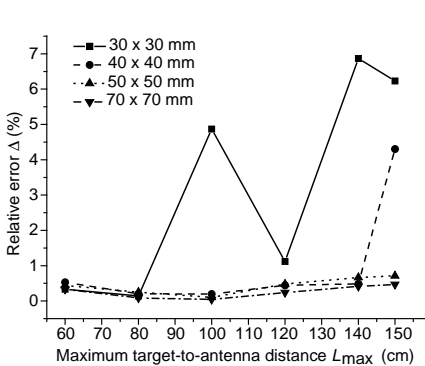

Figure 8. Relative error Δ in peak-to-peak amplitude determination versus the maximum target-to-antenna distance $L_{\max}$ for 30×30, 40×40, 50×50, and $70 \times 70\,\text{mm}$ brass square plates.

Figure 9. Measured displacement of a 40×40 brass square plate at different values of the maximum target-to-antenna distance $L_{\max}$.

comes a point where the condition (28) is no longer satisfied, and thus the phase unwrapping algorithm becomes inapplicable. This is illustrated in Figure 9, which shows the measured displacement of a 40×40 mm square plate at $L_{\max} = 60$ cm (Δ less than 1%) and 150 cm (a stepwise increase in Δ to 4.3%). As can be seen from the figure, at $L_{\max} = 150$ cm the measured time dependence of the displacement shows jumps. Eq. (28) suggests that the threshold value of $L_{\max}$ may be increased by increasing the sampling frequency.

4. CONCLUSION

This paper addresses the possibility of determining the displacement at an unknown reflection coefficient by microwave interferometry with the use of as few as two probes. The reflection coefficient at the location of the probes is expressed in terms of the currents of the semiconductor detectors connected to the probes as a root of a biquadratic equation, and it is shown that this expression is exact for reflection coefficients no greater than $1/\sqrt{2}$, while in the general case it allows the displacement to be determined to a worst-case theoretical accuracy of about 4.4% of the free-space operating wavelength λ_0. The proposed two-probe technique offers reasonable measurement accuracy for displacements several times as great as λ_0 (in $\lambda_0 = 3$ cm real-time measurements for a peak-to-peak vibration amplitude of 15 cm, the maximum error in the determination of the instantaneous relative displacement and the peak-to-peak amplitude was about 3 mm and about 1 mm, respectively). In hardware implementation, the proposed technique is far simpler than conventional techniques based on quadrature mixing [6, 7]. In particular, this technique dispenses with a quadrature mixer, whose nonlinear phase response presents a problem. As to conventional three-probe measurements [9], the reduction in the number of probes simplifies the design of the measuring waveguide section, alleviates the problem of interprobe interference and of selection of detectors with identical characteristics, and offers a higher sampling frequency due to the corresponding reduction in the required number of ADC channels.

REFERENCES

1. Cunha, A. and E. Caetano, "Dynamic measurements on stay cables of stay-cable bridges using an interferometry laser system," *Experimental Techniques*, Vol. 23, No. 3, 38–43, 1999.
2. Kaito, K., M. Abe, and Y. Fujino, "Development of a non-contact scanning vibration measurement system for real-scale structures,"

Structure and Infrastructure Engineering, Vol. 1, No. 3, 189–205, 2005.

3. Mehrabi, A. B., "In-service evaluation of cable-stayed bridges, overview of available methods, and findings," *Journal of Bridge Engineering*, Vol. 11, No. 6, 716–724, 2006.

4. Lee, J. J. and M. Shinozuka, "A vision-based system for remote sensing of bridge displacement," *NDT & E International*, Vol. 39, No. 5, 425–431, 2006.

5. Gentile, C., "Application of microwave remote sensing to dynamic testing of stay-cables," *Remote Sensing*, Vol. 2, No. 1, 36–51, 2010.

6. Kim, S. and C. Nguyen, "A displacement measurement technique using millimeter-wave interferometry," *IEEE Transactions on Microwave Theory and Techniques*, Vol. 51, No. 6, 1724–1728, 2003.

7. Kim, S. and C. Nguyen, "On the development of a multifunction millimeter-wave sensor for displacement sensing and low-velocity measurement," *IEEE Transactions on Microwave Theory and Techniques*, Vol. 52, No. 11, 2503–2512, 2004.

8. Tischer, F. J., *Mikrowellen-Messtechnik*, Springer-Verlag, Berlin, 1958.

9. Cripps, S. C., "VNA tales," *IEEE Microwave Magazine*, Vol. 8, No. 5, 28–44, 2007.

10. Chavez, S., Q.-S. Xiang, and L. An, "Understanding phase maps in MRI: A new cutline phase unwrapping method," *IEEE Transactions on Medical Imaging*, Vol. 21, No. 8, 966–977, 2002.

11. Hasar, U. C., J. J. Barroso, C. Sabah, and Y. Kaya, "Resolving phase ambiguity in the inverse problem of reflection-only measurement methods," *Progress In Electromagnetics Research*, Vol. 129, 405–420, 2012.

12. Silvia, M. T. and E. A. Robinson, *Deconvolution of Geophysical Time Series in the Exploration for Oil and Natural Gas*, Elsevier Scientific Publishing Company, Amsterdam, Oxford, New York, 1979.

13. Okubo, Y. and T. Uebo, "Experimental verification of measurement principle in standing wave radar capable of measuring distances down to zero meters," *Electronics and Communications in Japan (Part 1: Communication)*, Vol. 90, No. 9, 25–33, 2007.